From Department of Clinical Science, Intervention and Technology,
Division of Orthopedics and Biotechnology,
Karolinska Institutet, Stockholm, Sweden

BIMANUAL MOVEMENT CONTROL: INSIGHTS FROM GOLF BALL STRIKING

Fredrik Tinmark

Karolinska Institutet

Stockholm 2014

Published by Karolinska Institutet.
Printed by Åtta.45 Tryckeri AB

ISBN 978-91-7549-718-1

Bimanual Movement Control: Insights from Golf Ball Striking

THESIS FOR DOCTORAL DEGREE (Ph.D.)

By

Fredrik Tinmark

Principal Supervisor:
Toni Arndt, Ph.D., Professor
Biomechanics and Motor Control Laboratory
The Swedish School of Sport and Health Sciences, GIH, Stockholm, Sweden

Co-supervisor(s):
Maria Ekblom, Ph.D., Senior Lecturer
Biomechanics and Motor Control Laboratory
The Swedish School of Sport and Health Sciences, GIH, Stockholm, Sweden

Kjartan Halvorsen, Ph.D., Associate Professor
Division of Systems and Control
Department of Information Technology
Uppsala University, Uppsala, Sweden

Opponent:
John Rasmussen, Ph.D., Professor
Department of Mechanical Engineering and Manufacturing
Aalborg University, Aalborg, Denmark

Examination Board:
Svein Kleiven, Ph.D., Professor
Division of Neuronic Engineering
The School of Technology and Health
The Royal Institute of Technology

Louise Rönnqvist, Ph.D., Professor
Department of Psychology
Umeå University, Umeå, Sweden

Fredrik Ullén, Ph.D., Professor
Department of Neuroscience
Karolinska Institutet, Stockholm, Sweden

ABSTRACT

The aim of this thesis was to gain insight into the control of complex bimanual movements that are both fast and accurate. For this, skilled golf ball striking was used as a model in two experimental studies (I and III). The thesis also includes two methodological studies (II and IV), intended to assist in present and future investigation on bimanual movement control. Study I shows a common kinematic proximal-to-distal sequencing (PDS) pattern and speed-summation effect in skilled golf players of both genders. Using a common PDS movement strategy in golf ball striking at various endpoint speeds appears beneficial from mechanical and control points of view and could serve the purpose of providing both high speed and accuracy. In Study II a general expression for mobility was derived, which can be applied for extending the theory of mobility to double-handed grasping and manipulation. Study III found that kinematic contributions to endpoint velocity at slow, medium and fast test conditions were provided by the same subset of possible joint rotations. However, the specific subset differed between levels of expertise. The inertial behavior of the linkage arms-hands-club promoted movement parallel to and resisted movement orthogonal to the club path close to ball impact, at all endpoint speeds investigated. These findings extend previous knowledge regarding endpoint control in single-limb movements. Moreover, results regarding movement organization in Study I together with results in Study III regarding inertial behavior suggest the existence of limb configurations able to simultaneously exploit intersegmental dynamics and endpoint mobility in a proficient manner. To make the control of intersegmental dynamics in bimanual striking transparent, however, torques originating from segmental interactions should be determined. However, when hands are placed next to each other or are overlapping it becomes challenging to find placements for standard force sensors which allow separation of right and left hand forces without altering normal behavior. As partially explored in Study IV, pressure mapping of the right hand together with inverse dynamics calculations for the golf club can potentially provide an adequate solution.

LIST OF SCIENTIFIC PAPERS

I. **Tinmark F**, Hellström J, Halvorsen K, and Thorstensson A. Elite golfers' kinematic sequence in full-swing and partial-swing shots. *Sports Biomechanics* 9: 236 - 244, 2010.

II. Halvorsen K, **Tinmark F**, and Arndt A. The concept of mobility in single- and double handed manipulation. *Journal of Biomechanics,* Epub 18 Sept 2014.

III. **Tinmark F**, Arndt A, Ekblom M, Hellström J, and Halvorsen K. Endpoint control in a bimanual striking task: application to the golfswing. *Submitted.*

IV. **Tinmark F**, Arndt A, and Halvorsen K. Using Motion Analysis and Pressure sensitive sensors for determining normal forces when gripping a cylinder. *Manuscript.*

CONTENTS

LIST OF ABBREVIATIONS

CNS	Central nervous system
DOF	Degree of freedom
INT	Interaction torque
LJH	Leading joint hypothesis
MUS	Muscle torque
NET	Net torque
PDS	Proximal-to-distal sequencing

1 INTRODUCTION

With over 200 joints and 600 muscles within the human musculoskeletal system most motor tasks can be performed in multiple ways. However, each iteration must use one potential solution only. The need for a principle or control strategy is apparent. Experimental studies and computational models of voluntary upper limb movements have proposed that human motor behavior follow principles that mitigate the effects of several problems inherent in sensorimotor control, including signal delays and neural noise (Franklin and Wolpert, 2011). The experimental condition has traditionally involved a model of the upper limb as a planar three-link mechanism, even though more complex models can be found in recent studies about motor control of redundant mechanisms (Ambike and Schmiedeler, 2013). This thesis attempts to gain insight into the control of redundant mechanisms involving two upper limbs, using golf as model. This specific model differs from those of various single-limb tasks in the important aspect that the left and right upper limb manipulates the end-link through a bimanual grip.

1.1 SENSORIMOTOR TRANSFORMATIONS AND REDUNDANCY

Voluntary movements are under conscious control of the brain and organized around the performance of a purposeful task, whether it is to reach and lift a glass of water or to strike a golf ball. To control voluntary movement CNS uses a series of so-called sensorimotor transformations that convert incoming sensory information into motor commands (Kandel, 2013). Variability in the inputs and outputs of these transformations and inaccuracies in their internal representation lead to errors and variability in movement (Franklin and Wolpert, 2011) and underlie the decrease in movement accuracy with increasing speed (Woodworth, 1899). To achieve skilled motor performance the nervous system generally engages both feedforward and corrective feedback circuitry. Negative effects of feedback delays are reduced through the use of predictive processes (Franklin and Wolpert, 2011; Kandel, 2013).

The human musculoskeletal system is characterized by redundancy and as a consequence inverse transformations can generally not be uniquely specified. For example, the inverse kinematic transformation of a hand trajectory into joint angles can have many outputs based on the same input. However, humans are able to predict the effect of biomechanical factors and use these predictions to influence their control strategies in voluntary movements (Cos et al., 2011; Cos et al., 2012). Recent work suggests how biomechanical factors including interaction torques resulting from intersegmental dynamics (Dounskaia, 2005; Dounskaia et al., 2011; Sabes and Jordan, 1997; Sabes et al., 1998) and factors indirectly dependent on biomechanics such as variability and energetic costs (Harris and Wolpert, 1998; Jones et al., 2002), influence control strategies and might explain movement patterns shown when coordinating multiple degrees of freedom (DOFs).

1.2 INTERSEGMENTAL MOVEMENT

In movements that involve multiple body segments, rotation is not only caused by the torque created by gravity and muscles crossing a particular joint, but also by interaction torque (INT) from the motion of adjacent body segments. As the result of a comparatively high inertia and muscular mass of proximal body segments, the mechanical influence of proximal movement on distal joints is much higher than the corresponding influence of distal joint motion on proximal joints (Dounskaia, 2010; Hirashima et al., 2003; Putnam, 1993). Therefore, proximal-to-distal utilization of INT characterizes skilled single-limb movements with the purpose of maximizing speed in a distally held object or segment (Hirashima et al., 2007). Typical for the kinematics of such tasks is that proximal segments initiate rotation before distal ones, and that proximal segments begin to slow down before the distal segments have reached peak angular velocity. For a well-organized PDS motion, increments or carry-over effects of rotational velocity (speed-summation) from the proximal to distal segments could be maximized (Putnam, 1993).

An important aspect for minimizing endpoint variability is that a given torque or force can be more accurately generated by a stronger proximal muscle than a weaker distal one (Hamilton et al., 2004). Although proximal-to-distal sequencing (PDS) and proximal-to-distal utilization of INT primarily is associated with mechanical benefits when the speed requirement is high, such movement organization has also been found in skilled movement at relatively slow speeds. For example, in expert pianists (Furuya and Kinoshita, 2007) and in submaximal overarm throws performed by skilled baseball players (Hirashima et al., 2007). This is in agreement with findings reported in various reaching movements (Ambike and Schmiedeler, 2013; Dounskaia et al., 2011; Galloway and Koshland, 2002; Goble et al., 2007). Traditionally, major theories on motor control have regarded mechanical interactions between linked segments as by-products of the control strategy. An alternative interpretation suggests that the nervous system purposefully exploits the biomechanical properties of the limbs for movement organization. Dounskaia (2005) proposed that CNS use a hierarchical strategy in which a *leading joint* creates a dynamic foundation for motion of the entire limb. According to this theory, acceleration at the leading joint is produced by reciprocal muscle activity in a similar manner as during single-joint movements. In contrast, INT produced by leading joint motion generates a powerful mechanical effect on motion at other *subordinate joints*. The role of the subordinate joint musculature is to monitor the INT effect and to generate net torque (NET) that results in movement characteristics required by the task.

For reasons outlined above, INT is primarily produced by a proximally located leading joint. However, the location of the leading joint is also dependent on the task. In tasks requiring substantially smaller range of motion at the proximal than the distal joint, the mechanical influence of the proximal joint would be minor, and as a result, the distal joint may be more appropriate for the leading role (Dounskaia, 2010). The leading joint hypothesis (LJH) has been tested predominantly in reaching tasks with one arm, thus the location of *leading* and *subordinate joints* has not been determined for manipulation tasks involving a closed chain of

linked segments. Future research may reveal whether the LJH can be expanded beyond the notion of a single joint as the leading component of limb motion.

1.3 ENDPOINT CONTROL

1.3.1 Endpoint contributions

The kinematic contribution from each joint to the endpoint velocity of a multi-link structure is a function of joint velocity and configuration. Study of endpoint trajectory control in single-limb throwing and striking suggests that the difference in kinematic contribution from individual joint rotations can be extensive (Hirashima et al., 2007; Kim et al., 2009). In skilled overarm throwing the hand receives substantial contributions from some joint rotations and negligible contributions from others (Hirashima et al., 2007; Hirashima et al., 2008). Moreover, results suggest that joint rotations responsible for substantial kinematic contributions were either individual DOFs at *leading joints* or at *subordinate joints.* In the case of *subordinate joints,* those DOFs able to exploit interaction torques efficiently were major contributors (Hirashima et al., 2003; Hirashima et al., 2007; Kim et al., 2009). The study of throwing (Hirashima et al., 2007) also show that a single subset of DOFs may be employed among submaximal and maximal endpoint speeds.

1.3.2 Endpoint mobility

The possibility of modulating the inertia (and mobility), stiffness and damping of the endpoint/end-link is a feature of redundant manipulators such as the human arm (Hogan, 1984; Hogan, 1985). Modulation of stiffness and damping is made possible by co-activation of antagonists. Endpoint mobility represents the inertial behavior of the manipulator, and is the inverse of the inertia tensor for the endpoint (Hogan, 1985). The concept of mobility may reveal strategies of the motor control system in manipulation tasks. Redundant mechanisms such as the human arm can be configured in many different ways while performing the same task. The concept of mobility quantifies the degree to which a certain configuration promotes movement in certain directions, and resists (unwanted) movements in other directions. As Cos et al. (2012) pointed out, *"...the directions of maximal mobility/admittance may be viewed as valleys in a dynamic landscape that facilitate end-point stability perpendicular to movement direction and, as more control constraints are applied, the reduction of end-point variability becomes more significant. Movements along the minor axis exhibit a larger variability because of the lack of mechanical stability along the perpendicular direction. In other words, it is equivalent to moving along a ridge in the dynamic landscape and, hence, is most sensitive to perpendicular perturbations".*

A preference for maximal mobility parallel to hand path has been revealed while choosing between alternative reaching movements (Cos et al., 2011; Cos et al., 2012) and while reaching around obstacles (Sabes and Jordan, 1997; Sabes et al., 1998). Study of directional biases in a free-drawing task, however, suggests that the most preferred movement directions are those in which the need for active interference with INT is minimal (Dounskaia et al., 2011). In that particular task, directions of minimal inertial resistance were approximately

perpendicular to the most preferred directions. This poses a question whether manipulation tasks organized according to LJH, is compatible with limb configurations promoting end-point movement in wanted directions and resisting movement in other (unwanted) directions. Moreover, a derivation of the expression for mobility in two-arm manipulation has not been presented thus far. Accordingly, there is a need to extend the theory of mobility to bimanual grasping and manipulation.

2 AIMS

The overall aim of this thesis was to gain insight into the control of redundant mechanisms involving two upper limbs manipulating a tool through a bimanual grip.

The specific aims were:

I. To determine whether: (1) the golf swing performed by skilled golfers was organized in a common proximal-to-distal sequencing pattern when hitting golf shots both to maximal and submaximal distances; (2) a speed-summation effect is present, in term of increments of the segmental angular speed from pelvis to upper torso and from upper torso to hand; and (3) the sequencing pattern and/or the speed-summation were affected by gender or level of expertise.

II. To derive a general expression for mobility in double-handed manipulation.

III. To determine whether: (1) endpoint mobility is controlled to promote movement of the endpoint along its trajectory, and resist (unwanted) movement in other directions; (2) endpoint velocity contributions at impact would be invariant among golf shots at different speeds; and (3) endpoint control were dependent upon skill level.

IV. To explore and validate a partial method for force estimation at contact surfaces between the left and right hand in the bimanual grip as well as at contact surfaces between each hand and the golf club.

3 METHODS

3.1 PARTICIPANTS

Golf players with no self-reported recent injuries affecting their performance participated in Study I and Study III of this thesis (Table 1). Group 1 consisted of male professional players; groups 2 and 3 were composed by male and female amateurs ranked among the best in Sweden within their age category, respectively. In groups 4 and 5, male professional players and age matched male amateurs with an intermediate skill level participated. For application of the derived method in Study II, data from a single case (SC) in group 4 was used. Experiments in Study IV were performed by the test leader (thesis author). Written informed consent was obtained from parents or guardians of the players in case of underage, otherwise from the players themselves.

Table 1 Characteristics of the participants. Values for each group are reported as mean ± SD.

Study	Group	n	Age (years)	Height (m)	Mass (kg)	Hcp
I.	1	11 ♂	28 ± 5	1.82 ± 0.04	83 ± 6	NA
	2	21 ♂	17 ± 1	1.81 ± 0.05	74 ± 10	0 ± 2
	3	13 ♀	16 ± 1	1.68 ± 0.07	59 ± 9	-2 ± 2
III.	4	10 ♂	29 ± 6	1.81 ± 0.06	80 ± 5	NA
	5	10 ♂	30 ± 9	1.83 ± 0.06	77 ± 7	21 ± 5

3.2 APPARATUS

3.2.1 Studies I and III

Three-dimensional data were collected using a Polhemus Liberty electromagnetic tracking system (Polhemus Inc., Colchester, VT, USA), with sampling frequencies at 120 (Study III) and 240 Hz (Study I). According to the manufacturer, the static accuracy is 0.076 mm RMS for sensor position and 0.15° RMS for sensor orientation. Values for dynamic accuracy of 0.71 mm RMS were reported by Nafis et al. (2006) for sensor positions at distances up to 0.46 m from the transmitter. The system used in Study I and Study III was compared to an optoelectronic tracking system (8-camera ProReflex MCU1000 System, Qualisys AB, GBG, Sweden). In full-swing shots using a steel-shafted 5 iron, the Bland-Altman (Bland and Altman, 1986) mean difference for hand angular speed was 24 deg/s (limits of agreement: -126, 174). The magnitude of this difference varied with angular speed, at minimum and maximum mean angular speeds the difference between the systems was 4 and 17 deg/s, respectively (Tinmark, Hellström and Halvorsen, unpublished data).

3.2.2 Study IV

3.2.2.1 Optoelectronic tracking system

An optoelectronic 3D motion capture system with twelve infrared cameras (Oqus 4 camera series, Qualisys AB, Gothenburg, Sweden) was used to collect trajectories of spherical retro-reflective markers (12 mm diameter). The camera system was calibrated according to the manufacturer's guide lines using a 0.375 m wand. The standard deviation of the reconstructed wand length was 0.32 mm within the measurement volume.

3.2.2.2 Pressure distribution measurement system

Pressure distribution data were collected with the capacitive sensor matrices Elastisens S2073_11 (226 x 56.5 mm) and Elastisens S2076 (113 x 113 mm) (Pliance-X System, Novel GmbH, Munich, Germany) attached around the circumference of a cylinder. The spatial resolution of the two sensor matrices were 0.5 sensors/cm^2 (low resolution (LR) sensor) and 2.0 sensors/cm^2 (high resolution (HR) sensor) respectively.

3.3 DATA ACQUISITION

3.3.1 Study I

Players first performed a warm-up session of approximately 10 minutes that involved golf shots to varying distances. Then, three sensors (23x28x15 mm, 9.1 g) were attached to each player at the following locations to monitor the motion of pelvis, torso and hand: the lumbo-sacral joint (hereafter referred to as pelvis); (2) between the shoulders at the level of the third thoracic vertebra (torso); and (3) the dorsal part of the leading hand (hand). For each segment, the specific sensor placement was based on minimizing movement between sensors and underlying bone as well as the interference with the players´ regular motion. The pelvis and torso sensors were mounted on a harness and the hand sensor was secured with a golf glove. Location of marker clusters representing sensors is presented in Figure 1. To minimize metal interference the capture volume for the electromagnetic system was distanced from any structural metals, except the players' steel golf shafts.

The measurements started with a static trial, in which the players were required to stand in the anatomical position parallel to the shot direction. Then spatiotemporal data were collected under 5 different test conditions. Test conditions 1-3 consisted of partial shots with a wedge to targets at 3 discrete distances, 40, 55 and 70 m. The order was such that players had to hit the ball progressively farther for each shot. This procedure was repeated three times. Thus the players did not aim for the same target twice in a row, except when the ball landed closer to another target (target zone radius = 7.5 m). Such a trial was discarded and followed by a new trial to the same target. Test conditions 4-5 were 3 consecutive full-swing shots with a 5 iron and a driver, respectively, for maximal distance. Players used their own clubs. Type of wedge was chosen individually and governed by the criteria that it should be the most lofted club with which the participant repeatedly could hit farther than 70 m with a full-swing shot. Plastic cones or flags were used as targets for the partial shots.

The orientation of the right-handed orthogonal global coordinate system was such that the positive x-axis pointed parallel to the shot direction, the positive z-axis vertically upwards, and the positive y-axis forward from the right-handed golfer. The shots were performed from an artificial turf mat positioned next to the transmitter. The experimental set-up yielded a measurement space, in which the distance from transmitter to sensors ranged from 0.16 – 1.41 m during recordings.

3.3.2 Study III

A warm-up session corresponding to that in Study I was first performed. Then seven sensors were attached at the following locations: (1) the lumbo-sacral joint (hereafter referred to as pelvis); (2) between the shoulders at the level of the third thoracic vertebra (torso); (3) posteriorly on the left humerus immediately proximal to the left elbow joint (left upper arm); (4) posteriorly on the right humerus immediately proximal to the right elbow joint (right upper arm) ; (5) the dorsal part of the left hand (left hand); (6) the dorsal part of the right hand (right hand) and (7) the proximal part of the club shaft – below the grip (club). The specific sensor placement was chosen by the same criteria as in Study I, that is, to minimize movement between sensors and underlying bone and to minimize interference with the players´ regular motion. The pelvis, torso and arm sensors were secured with a harness and the hand sensor was secured with a golf glove. In addition, arm and hand sensors were secured with double-sided adhesive tape. The shaft sensor was locked with a small plastic clamp. Following sensor attachment, players performed an additional 5 minutes of warm-up in order to habituate themselves to the sensors and harnesses. Then, a static trial and the digitization of 26 anatomical landmarks (virtual landmarks) were performed. Locations of virtual markers, calculated joint centers and marker clusters representing the sensors are presented in Figure 1.

Spatiotemporal data were collected under 3 different test conditions. Test conditions 1-2 consisted of partial shots with a wedge to targets at two discrete distances, 25 and 55 m. Test condition 3 consisted of full-swing shots in the same direction for maximal distance (>75 m). Test conditions 1-3 are hereafter referred to as slow, medium, and fast. Players hit the ball progressively farther for each shot. This procedure was repeated 3 times. Thus, the players did not aim for the same shot distance twice in a row, except when the ball landed closer to another target (target zone radius = 5 m). Such a trial was discarded and followed by a new trial to the same target.

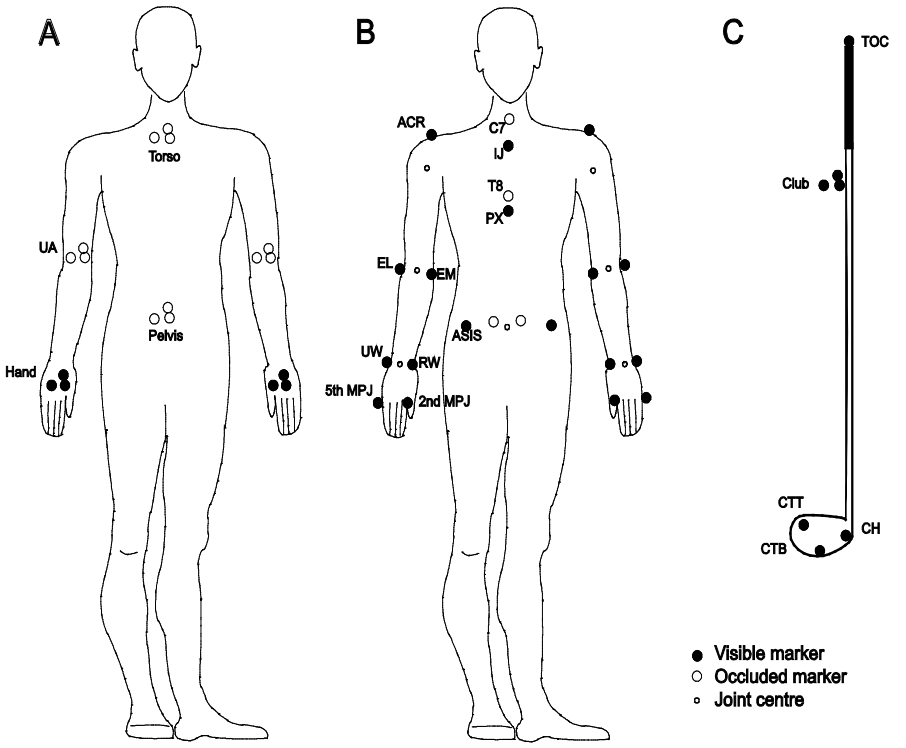

Figure 1 A: Locations of marker clusters representing sensors at pelvis, torso, upper arm (UA) and hand. B: Locations of calculated joint centers and locations of virtual markers: acromion (ACR), insicura jugularis (IJ), processus xiphoideus (PX), C7, T8, ASIS, PSIS, lateral elbow (EL), medial elbow (EM), radial wrist (RW), ulnar wrist (UW), 2nd and 5th metacarpophalangeal joint (MPJ). C: Location of marker cluster representing club sensor and locations of virtual markers: top of club (TOC), club heel (CH), club toe bottom (CTB) and club toe top (CTT). For markers placed bilaterally, names/abbreviations are shown only for markers on the right side of the body.

3.3.3 Study IV

As a consequence of the multiplexing technology that sequentially scans the sensor elements, there is a trade-off between maximum scanning frequency and the number of active sensor elements (Lemerle et al., 2008). For our application a minimum scanning frequency of 140 Hz was decided upon. Consequently, the number of sensor elements and the resulting sensor measurement area of the HR sensor (2.0 sensors/cm^2) did not allow pressure-mapping of both hands simultaneously. Based on the assumption that tangential forces at the hand-handle interface are relatively small for the right hand throughout the golf swing compared to tangential forces for the left hand, we decided to perform all experimental tasks using the right hand only. A relevant amplitude and range of forces for the application to be tested must be defined. In this study pressure distribution data and internal force data for the right hand, when performing golf swings with a wedge at three different speeds, were used to plan two sets of experimental tasks. In the first set of tasks, a higher range of internal forces was replicated by raising and lowering an external weight of 3 kg using an instrumented cylinder (Figure 2). In the second set of tasks, a lower range of internal forces was replicated by raising and lowering an external weight of 1 kg. Grip pressure on the cylinder was then

regulated using external feedback to replicate the range of internal forces in medium and fast golf swings without changing the external weight. In addition to the dynamic trials (D) where the cylinder and external weight were raised and lowered repetitively, both sets of tasks also included static trials (S) where the instruction was to hold the cylinder and external weight as still as possible. To study the effect of altered tangential forces, both static trials (SG) and dynamic trials (DG) were repeated with ultrasonic gel applied to the right hand and sensor surface. All trials were performed with the right hand only; they were repeated three times and included three raising-lowering cycles. Pressure distribution and internal force data were displayed and monitored in real time during data collection.

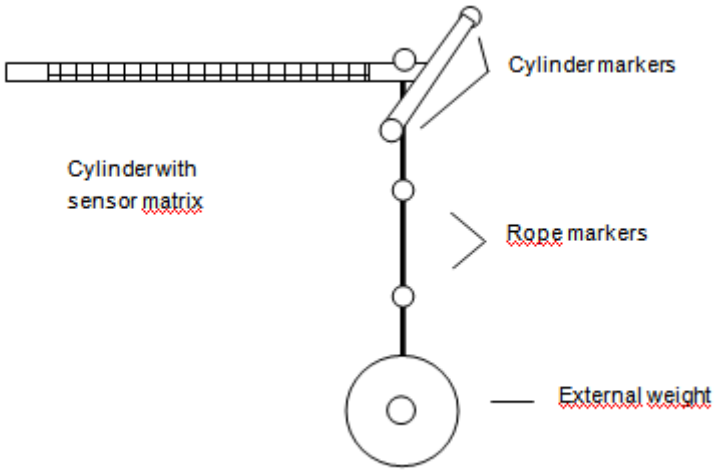

Figure 2 Cylinder with sensor matrix, retro-reflective markers, and external weight.

3.4 MECHANICAL MODEL

3.4.1 Study III

The upper body was represented by 8 rigid body segments: pelvis, upper torso, upper arms, forearms and hands. Two bilateral open chains corresponding to the left and right arm described the kinematics of the body and the club. Each chain consisted of the upper arm, forearm, hand and club segments. Twenty-six digitized landmarks were used to define segment lengths, orientation of local coordinate frames and joint centers (Figure 1B and 1C). The model was constrained to 41 degrees of freedom (DOFs). The pelvis segment was defined to be the root segment of the kinematic chains, with 6 DOFs. The joint between the pelvis and torso was defined as a spherical joint with 3 DOFs and center of rotation at the middle of the asis-psis plane. Both arms had the same number of DOFs: 6 DOFs for the shoulder joints, 2 DOFs (flexion/extension and pronation/supination) for the elbow joints, and

2 DOFs for the wrist joints (flexion/extension and ulnar/radial deviation). Finally, the connection between the hand and club was described with 6 DOFs.

The two open kinematic chains corresponding to the left and right arms both contained the club segment as the most distal segment. The same motion data of the club was used in the inverse kinematics calculations for both kinematic chains, but no hard constraint was enforced to make the computed movement of the "left" and "right" club exactly the same.

3.4.2 Study IV

A model of the instrumented cylinder (Fig. 2) containing a list of all cells in the sensor mat, their position in a local coordinate system, and their normal vector, was fitted to marker data by using point correspondence . The positions in 3D, with respect to the marker triad on the handle, of the center of six (LR sensor) and nine (HR sensor) cells were indicated with a pointer device. The normal force vector for each cell was computed by multiplying a radial unit vector (origin at the center of each cell) with pressure data and cell area. The resultant force was computed by adding all normal force vectors. To examine the validity of using motion capture and pressure sensitive sensors to estimate the resultant normal force, values computed by multiplying the combined mass of the cylinder and external weight by the acceleration and gravity were used as reference. Root mean square error (RMS error), coefficient of variation (CV) and angle between vectors (direction error) were utilized as measures of differences between the two sets of force values in each trial. Calculations were performed in Matlab (Version 7.14.0, The Mathworks, Inc., Natick, USA).

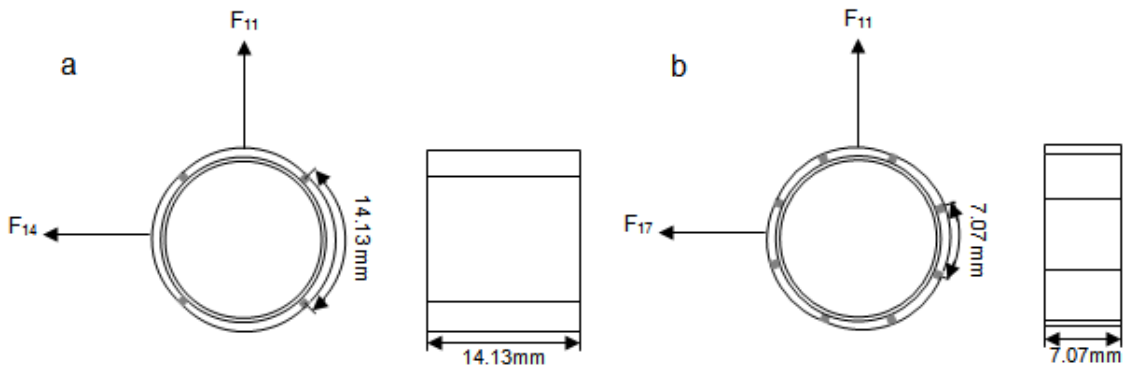

Figure 3 Cross sectional view and side view of the first row in the 3D model for: (a) the cylinder with the low resolution sensor matrix; and (b) the cylinder with the high resolution sensor matrix.

3.5 DATA PROCESSING

3.5.1 Study I

The raw data were smoothed using a second-order, bidirectional, low-pass Butterworth filter with cut-off frequency set at 14 Hz, determined through residual analysis (Winter, 2005). Due to the non-planar nature of the golf-swing (Coleman and Anderson, 2007; Coleman and Rankin, 2005), the angular velocity for each segment was calculated from the finite difference of the rotation matrix expressing the orientation of the segment with respect to the laboratory reference frame in three-dimensional space (Kinzel et al., 1972). This vector is expressed in the laboratory frame and is independent of the choice of local segment frames. The magnitude of this vector is referred to as segment angular speed. Segment angular speeds for each player and test condition were represented by the mean of 3 successfully performed trials. The swing was divided into 2 phases defined by 3 events. The first event (start of backswing) was defined as the frame where the linear velocity of the hand sensor crossed a threshold value of -0.2 m/s in the global x-direction. The second event (top of backswing = start of downswing) was determined as the first occurrence of minimum angular speed for any of the 3 segments following start of backswing. The third event (end of downswing) was determined as the frame where the hand returned to the same global x-position as at start of backswing. To determine sequencing pattern, times for minimum and maximum (peak) segment angular speeds were analysed. Visual3D v.3.90 Beta and v.3.99 (C-Motion, Inc., Rockville, MD, USA) commercial software packages were used for all calculations of kinematic and temporal parameters.

3.5.2 Studies II and III

3.5.2.1 Endpoint contributions

The state of the model is a set of joint angles collected in the vector q, and corresponding velocities $\dot{q}$. The state was estimated from motion data using an extended Kalman filter (Anderson and Moore, 1979; Halvorsen et al., 2008). The state estimate (Kalman) filter paradigm makes it possible to improve the estimated movement of the body by utilizing knowledge of the error covariances of the motion capture data and knowledge of how fast changes occur in the different degrees of freedom. These assumptions are represented by the measurement noise- and process noise covariance matrices, respectively. For the current application we used knowledge of the typical peak acceleration of each DOF during the downswing phase to set the values for the diagonal elements of the process noise covariance matrix. The process noise was assumed to be independent for different DOFs, and hence diagonal. For the measurement noise we assumed the noise to be independent and have the same variance for each measured point coordinate. Thus, the measurement noise covariance was assumed to be a scalar variance parameter multiplying the identity matrix. One scalar tuning parameter remained, i.e., the measurement variance, which determines the smoothness of the estimated time series for the DOFs. This parameter was determined experimentally by comparing marker trajectories reconstructed from the model with marker trajectories obtained

by simple low-pass filtering of the original trajectory. A variance parameter corresponding approximately to low-pass filtering with a cut-off frequency of 15 Hz was chosen. Mean residual was used as measure of the differences between 3D marker coordinates predicted by the model and marker coordinates that were recorded. The mean residual for all trials and markers was 3.06 mm. Corresponding values for individual markers ranged between 0.53 mm and 6.99 mm.

The contribution from each joint angular velocity to the velocity of the endpoint (the clubhead) was calculated by differentiating the mapping from state vectors to the position of the endpoint, and using the chain-rule:

$$p = g(q), \tag{1}$$

$$\dot{p} = J(q)\dot{q}. \tag{2}$$

where $J(q)$ is the Jacobian of the kinematic model. At each sampled instance of time, the contribution from the angular velocity of a given degree of freedom was calculated assuming the rest of the joints in the kinematic model to be momentarily fixed, with zero angular velocity. The single remaining angular velocity gives a certain velocity at the endpoint. The sum of these endpoint velocities contributed by all the degrees of freedom provides the actual velocity of the endpoint.

3.5.2.2 Endpoint mobility

The endpoint mobility describes, in a sense, how easy it is to accelerate the endpoint in different directions, and is defined as the inverse of the inertia matrix of the end point. The mass matrix is in general neither isotropic nor constant. It depends on the configuration of the mechanism. For single-handed manipulation, the mobility matrix is calculated as:

$$W(q) = J(q)Y(q)J^T(q) \tag{3}$$

where $Y(q)$ is the inverse of the generalized inertia of the mechanism, i.e. the mobility matrix for the complete linkage. For double-handed manipulation the calculation involves inverting the apparent mass matrix of the end-point. The apparent masses of the two arms and the mass of the club are added for the case of a firm grip. The expression for mobility then becomes:

$$W(q) = (M(q) + M_0)^{-1} = ((J_L Y_L(q) J_L^T)^{-1} + (J_R Y_R(q) J_R^T)^{-1} + M_0)^{-1} \tag{4}$$

where $M(q)$ refers to the apparent mass of the two arms and M_0 to the inertial matrix of the golf club. Subscripts *L* and *R* refer to the left and right arms, respectively. A detailed derivation of this expression is found in Study II.

Endpoint mobility was calculated for 2 endpoints and 3 different models. The first endpoint (midhands) was located between the hands at the center of the grip and the second endpoint (clubhead) was located in the middle of the clubhead. The 3 different models corresponded

to: (1) left arm and club; (2) right arm and club; and (3) left arm, right arm and club. The left and right arm models contained the same DOFs used in calculations of endpoint velocity contributions. The connection between hand and club was assumed to be rigid. Virtual landmarks were used to define segment lengths, orientation of local coordinate frames and joint centers (Fig. 1b and 1c). Segment inertia parameters were obtained from de Leva (1996).

Four endpoint mobility measures were derived: (1) degree of alignment; (2) eccentricity; (3) endpoint mobility along path; and (4) endpoint mobility normal to path. Degree of alignment is the 3D angle between the major axis of the mobility ellipsoid and endpoint path (the mobility ellipsoid is derived by calculating the eigenvalues and eigenvectors of the mobility matrix). Eccentricity is the relative separation of the first and second singular value of the mobility matrix: $(\sigma_1 - \sigma_2)/ \sigma_1$. For an ellipsoid collapsed to one dimension, this value is 1. For a completely round, or squeezed (round but flat) ellipsoid the value is 0.

3.5.3 Study IV

The normal force vector for each cell was computed by multiplying a radial unit vector (origin at the center of each cell) with pressure data and cell area. The resultant force was computed by adding all normal force vectors. To examine the validity of using motion capture and pressure sensitive sensors to estimate the resultant normal force, values computed by multiplying the combined mass of the cylinder and external weight by the acceleration and gravity were used as reference. Root mean square error (RMS error), coefficient of variation (CV) and angle between vectors (direction error) were utilized as measures of differences between the two sets of force values in each trial. Calculations were performed in Matlab (Version 7.14.0, The Mathworks, Inc., Natick, USA).

3.6 STATISTICAL ANALYSIS

3.6.1 Study I

Statistics were calculated using SPSS 15.0 (SPSS, Inc., Chicago, IL, USA). Shapiro Wilk´s W test was applied to test normality in the distribution of data. Differences in time for minimum and maximum segment angular speeds, magnitudes of maximum segment angular speeds, and increments in maximum segment angular speed, were analyzed in separate repeated-measures ANOVAs with group as between-subjects factor, and test condition and body segment as within-subjects factors. To isolate differences in repeated-measures ANOVAs, pre-planned comparisons were conducted using paired *t*-tests with Bonferroni correction. Since data did not conform to the assumption of sphericity, *p*-values for the ANOVAs were Greenhouse-Geisser adjusted. Significance level for all tests was set at $p < 0.05$.

3.6.2 Study III

Statistics were calculated using Statistica 12 (StatSoft Inc., USA). Differences in endpoint velocity contributions at estimated impact were analyzed in separate repeated-measures

ANOVAs with test condition as within-subject factor and group as between-subject factor. Repeated measures ANOVAs were also used for analyzing differences in alignment of the major axis of the mobility ellipsoid with the endpoint velocity vector, and for analyzing differences in the eccentricity of the mobility ellipsoid. Pair-wise comparisons were conducted using Tukey HSD tests. In addition, pre-planned one-tailed t-tests were conducted to test whether the major axis of the mobility ellipsoid was better aligned with the endpoint velocity vector than the other two axes (3D angle less than 45°). Significance level was set at $P < 0.05$.

3.6.3 Study IV

Root mean square error (RMS error), coefficient of variation (CV) and angle between vectors (direction error) were utilized as measures of differences between the two sets of force values in each trial.

4 RESULTS AND DISCUSSION

4.1 INTERSEGMENTAL MOVEMENT

4.1.1 Temporal characteristics

Results regarding temporal characteristics of pelvis and torso motion (Table 2) in full-swing shots are consistent with previous study of pelvis and upper torso motion, estimated by determining transverse plane rotations (Burden et al., 1998; Cheetham et al., 2001; Fujimoto-Kanatani, 1995). The proximal-to-distal temporal order of torso and hand segments has not been reported earlier, but is consistent with findings regarding the order in which the shoulder and wrist joints attain maximum angular speed (Milburn, 1982; Zheng et al., 2008). Thus, the current results confirm that PDS is used by skilled golf players in full-swing shots.

Table 2 Mean (± SD) times for minimum and maximum angular speed (% of downswing duration) for each of the 3 body segments and for each of the 5 test conditions. Values for all 3 groups are combined (n=45).

	Body segment		
Variable & Test condition	**Pelvis**	**Torso**	**Hand**
Time for minimum speed			
40 m	0.8 ± 4.0[a]	4.3 ± 5.3	4.9 ± 4.0
55 m	1.4 ± 4.9[a]	3.8 ± 4.0	4.7 ± 4.3
70 m	1.3 ± 4.5[a]	3.6 ± 3.5	4.5 ± 3.6
5iron	1.3 ± 4.8[a]	3.6 ± 3.9	4.6 ± 3.6
Driver	1.4 ± 4.3[a]	4.3 ± 4.9	5.5 ± 3.8
Time for maximum speed			
40 m	84.6 ± 13.3[a]	92.3 ± 10.3[b]	103.6 ± 3.8
55 m	80.6 ± 8.8[a]	90.3 ± 10.0[b]	103.6 ± 3.4
70 m	79.0 ± 9.6[a]	87.2 ± 9.9[b]	103.3 ± 3.7
5iron	75.1 ± 8.3[a]	85.2 ± 12.2[b]	110.6 ± 13.0
Driver	74.3 ± 7.7[a]	84.6 ± 10.5[b]	102.5 ± 2.8

[a] *Significantly different from torso and hand*

[b] *Significantly different from hand*

The novel finding that PDS is present also in shots at relatively slow club speeds is consistent with previous study of single-limb tasks (Furuya and Kinoshita, 2007; Hirashima et al., 2007). Hirashima et al. (2007) observed that skilled throwers use proximal trunk and shoulder muscles to create beneficial interaction torques for more distal joint rotations at both submaximal and maximal ball speeds. Ball speed regulation was explained by altered

proximal muscle torques and distal interaction torques, whereas no difference in distal muscle torques was present. These authors hypothesized that this strategy can be used to improve accuracy, referring to the finding by Hamilton et al. (2004) that a given torque or force can be more accurately generated by a stronger proximal muscle than a weaker distal one. This notion is in line with the movement organization shown in goal-directed reaching movements (Yamasaki et al., 2008), which can be explained by optimal control models that generate movements in a way that minimize endpoint variability (Harris and Wolpert, 1998; van Beers et al., 2004). A similar reasoning concerning the role of PDS in golf shots would require kinetic data, including inter-limb dynamics considering that golf is a bimanual striking task. However, the use of interaction torques for generating club speed was indicated by the present temporal relation, where the distal segment accelerated while the more proximal segment was decelerating, as well as by the proximal-to-distal increment in the magnitude of segment angular speeds (Figure 4 and 5).

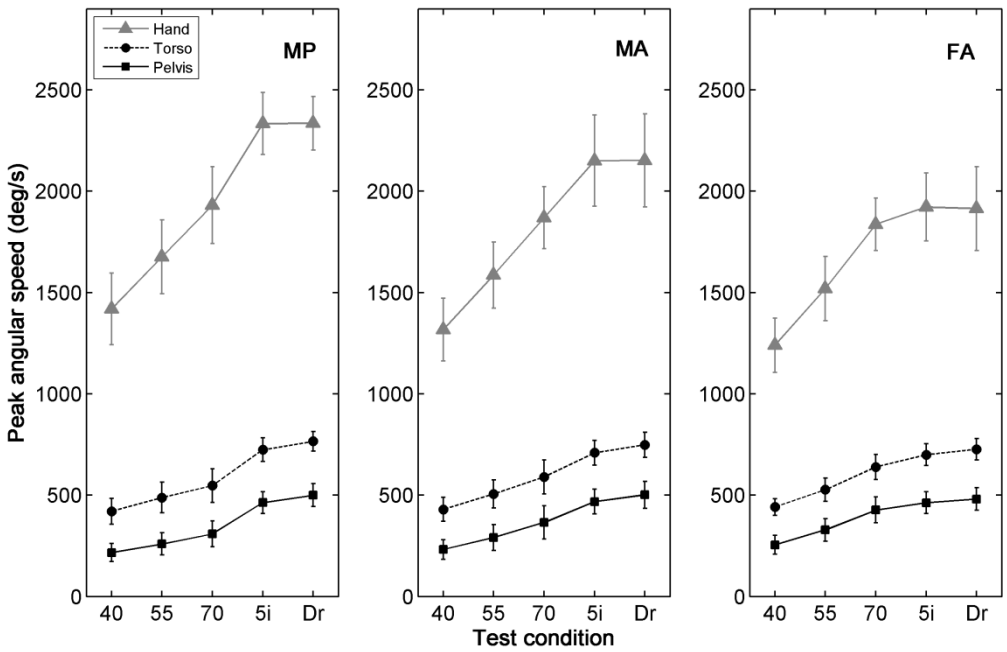

Figure 4 Group mean values (±SD) for maximum segment angular speed (deg/s) during the downswing for the pelvis, torso and hand segments in the male professionals (MP), male amateurs (MA) and female amateurs (FA) under the 5 different test conditions (cf. Methods).

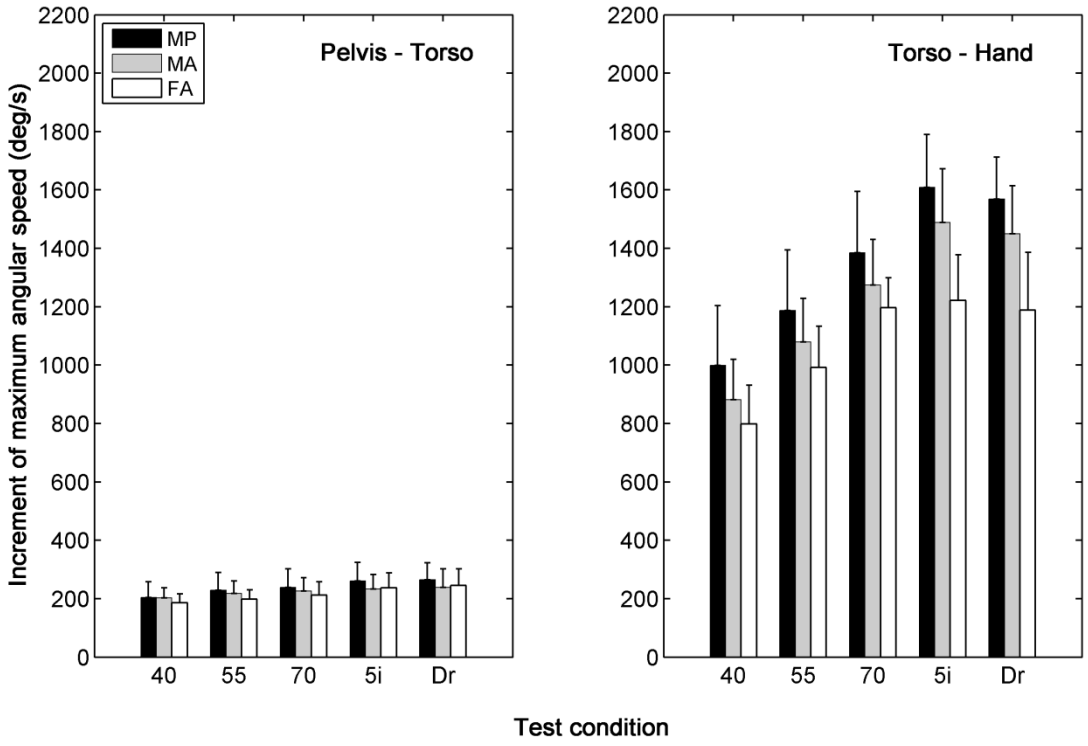

Figure 5 Group mean values (±SD) for increment of maximum segment angular speed (deg/s) during the downswing for pelvis to torso (left) and from torso to hand (right) in the male professionals (MP), male amateurs (MA) and female amateurs (FA) under the 5 different test conditions (cf. Methods).

In conclusion, the observed temporal relation of segment kinematics suggests a common PDS organization in both partial and full-swing shots for skilled golfers. The temporal relation and increment in segment angular speed indicate that the players utilized interaction torques in a proximal-to-distal manner. To establish the locations of *leading* and *subordinate* joints – a method which allows separation of right and left hand forces without altering normal behavior is called for. Such a method was partially explored in Study IV.

4.1.2 Separation of left and right hand forces

Figures 6 and 7 show the RMS error, CV of the force magnitude and direction error values for the estimate of the resultant normal force. Sensor resolution has a large impact on both magnitude and direction of the measured normal force vector. The CV of the force magnitude for all trials combined was approximately 0.71 when using a capacitive sensor matrix with 0.5 sensors/cm^2, and 0.37 when using a capacitive sensor matrix with 2.0 sensors/cm^2. The corresponding direction errors were 35° and 15°, respectively. The results for all trials combined suggest that accuracy may be too low for most applications. However, lowering friction by using gel at the hand-handle interface improved the estimate of magnitude and direction of the resultant force vector substantially in the set of tasks using an external weight of 3 kg (Fig. 6). Here, the CV of the force magnitude was 0.25 and the direction error was 10°. Applying gel had small or negligible effect in the set of tasks using an external weight of 1 kg (Fig. 7). This indicates that a high ratio between normal and tangential forces is essential

for accuracy. A further test supporting the conclusion that tangential forces influence the estimation of the resultant normal force vector was performed. Repeating one static trial with only the left hand, the average length of the resultant normal force vector was not affected substantially but direction was reflected about the vertical plane (results not shown).

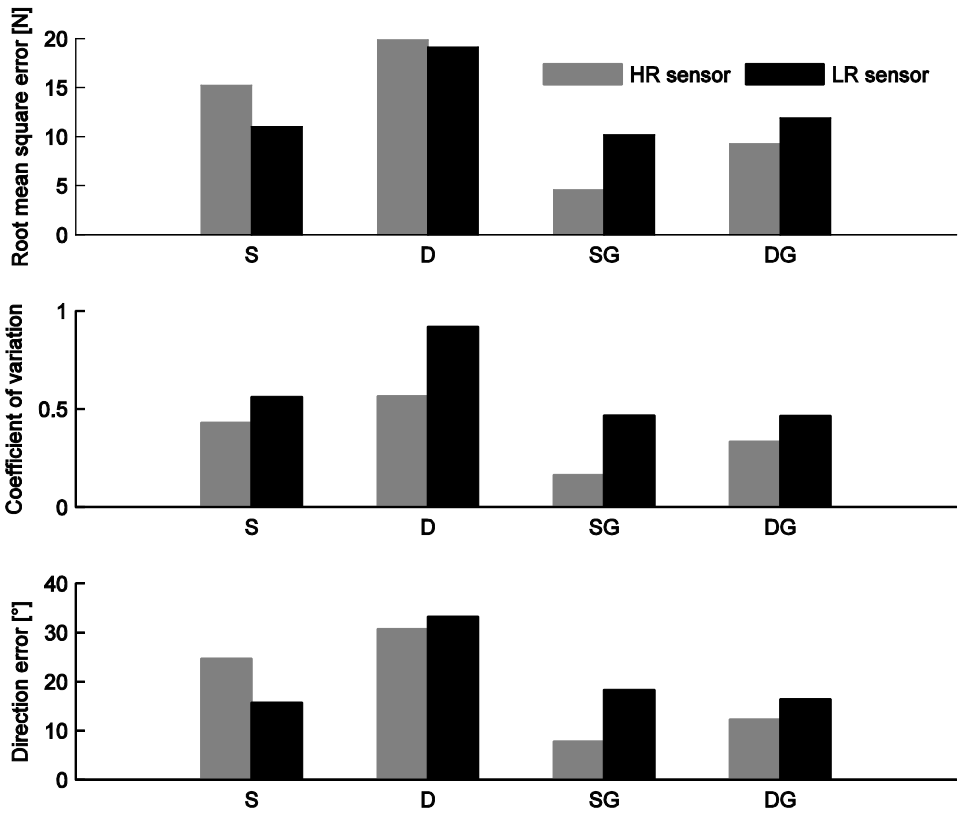

Figure 6 Root mean square error, coefficient of variation, and direction error for the two sensors in four tasks: static (S); dynamic (D); static with gel (SG); and dynamic with gel (DG).

The improved estimate of the resultant normal force vector when lowering the friction by applying gel to the hand-handle surfaces is consistent with findings reported by Lemerle et al. (2008). In addition to studying the effect of lowering friction by applying gel, they also investigated the effect of using known static vertical loads on sensor strips and sensor cells exposed to horizontal pulling forces. With vertical loads up to one-third of the normal forces, they reported a maximal error of 7% resulting from the tangential forces (Lemerle et al., 2008). A limitation of the current study is that the actual tangential forces were not measured. Moreover, the tangential forces in the model application (golf swing) are not well known either. Consequently, only subjective judgments of the magnitude of these forces and the agreement between the laboratory setting and the real task can be made. Here, golf shots were performed by an elite golfer with and without gel applied to surfaces where fingers of the right hand are in contact with the cylinder, in order to do a qualitative assessment. Golf shots

with gel at the hand-handle interface for the right hand could be performed without notably altering the experience of normal behavior, suggesting that tangential forces are small in both cases. However, the magnitude of right hand tangential forces in the golf swing should be further investigated.

In conclusion, results imply that a high ratio between normal and tangential forces in addition to a sensor matrix with high spatial resolution is required to obtain acceptable errors when estimating normal forces at the hand-handle interface when gripping a cylinder. Potentially, pressure mapping of the right hand together with inverse dynamics calculations for the golf club can provide an adequate solution to separate right and left hand forces either in the golf swing or similarly in other sport or tool applications. However, using the method presented in this study, a minimum CV of 0.25 and a minimum direction error of 10° should be expected.

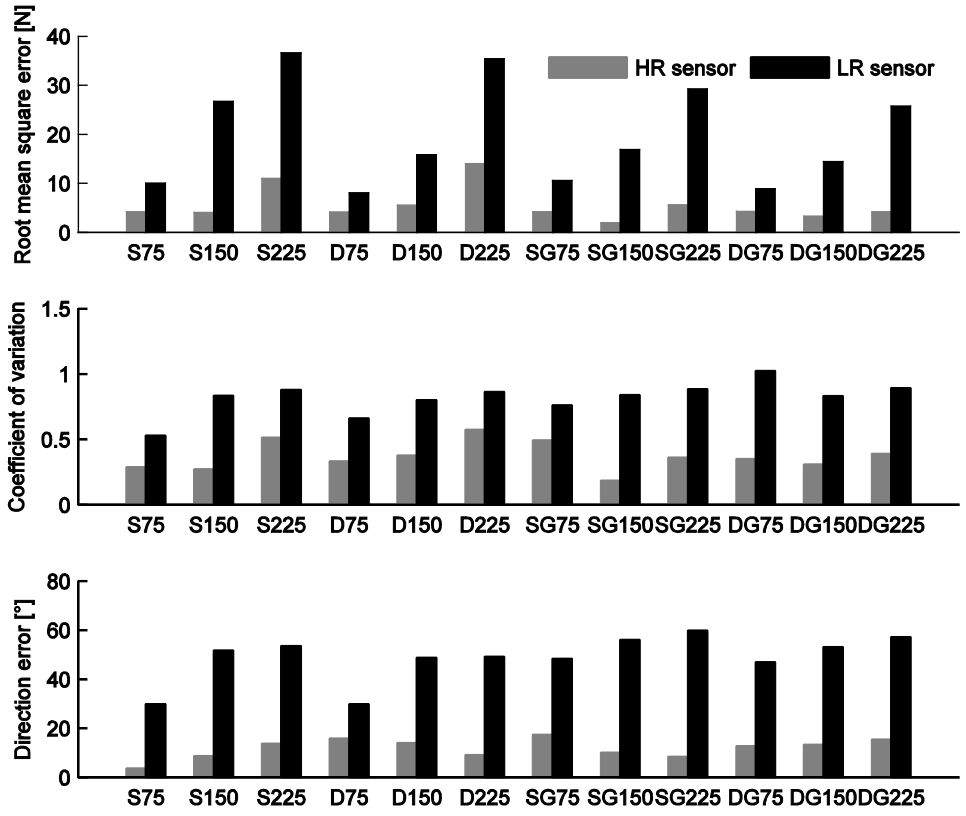

Figure 7 Root mean square error, coefficient of variation, and direction error for the two sensors in twelve tasks: static (S); dynamic (D); static with gel (SG); and dynamic with gel (DG). 75, 150, and 225 indicate internal force values [N] achieved by regulating grip pressure.

4.2 ENDPOINT CONTROL

4.2.1 Endpoint contributions

Consistent with findings in overarm throwing several joint rotations made negligible contributions to endpoint speed at impact (Hirashima et al., 2007). Statistical analysis to reveal DOFs involved in speed regulation was therefore limited to a subset of the 20 DOFs with the greatest contributions. These 20 DOFs were the same for both groups and explained 96.7% of endpoint speed. For 16 of these 20 DOFs, repeated-measures ANOVAs showed a main effect of test condition on contributions to endpoint velocity (Fig. 8). The contributions from this subset of 16 DOFs explained 97 to 99% of the mean change in endpoint velocities between test conditions.

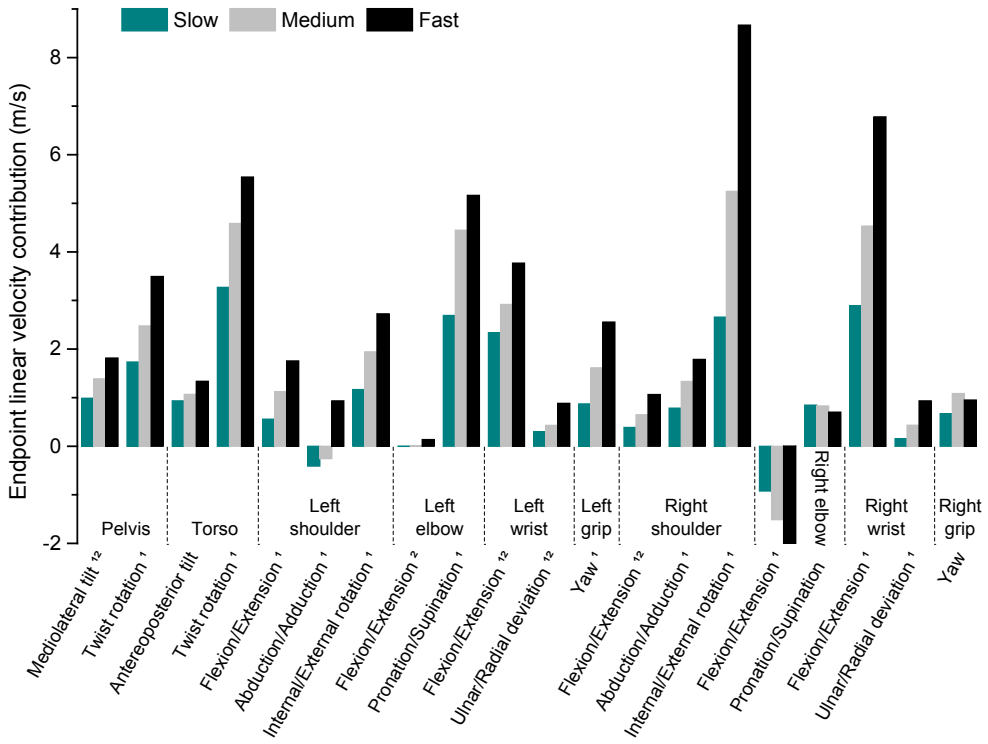

Figure 8 Mean contributions to endpoint linear velocity (m/s) for each of 20 DOFs and for each of 3 test conditions at estimated impact for both groups combined (n=20). ¹ Main effect of shot condition. ² Interaction between shot condition and group.

Results regarding endpoint velocity contributions were equally valid for both advanced and intermediate players, apart from 4 joint rotations in the subset contributing to endpoint speed (Figure 3 and 4 in Study III). This exception may reflect the previously established fact that efficient exploitation of interaction torques is skill dependent. The differences in distal joint contributions are presumably associated with differences in co-contraction rather than in

segmental configuration. Hereafter, results common to both intermediate and advanced players are discussed.

For the pelvis and torso, the highest contribution for both groups at estimated impact was provided by twist rotation. These results are compatible with those from studies of unconstrained overarm throws and horizontal arm swings (Hirashima et al., 2007; Kim et al., 2009). Whereas pelvis and trunk velocities were lower compared to the most distal joints, clubhead velocity depends on the distance from the axis of rotation, therefore motion at the pelvis and trunk was amplified to a larger degree. Moreover, results for left shoulder flexion/extension and left wrist flexion/extension are consistent with those reported in horizontal arm swings performed with the non-dominant arm (Kim et al., 2009). However, Kim et al. (2009) reported that elbow extension was a major contributor to endpoint velocity whereas in the golf swing only negligible contributions from left elbow extension were found. Considering that the bilateral axis of the left elbow joint in golf has similar orientation with respect to endpoint path as in horizontal arm swings, substantial contributions from elbow extension to endpoint velocity could be expected. Presumably, keeping the left arm relatively straight throughout the golf swing facilitates ball contact and outweighs any potential endpoint velocity gains attainable by elbow extension. Among right arm (trailing arm) DOFs, shoulder internal/external rotation and wrist flexion/extension contributed the most at estimated impact. This is consistent with findings for right overarm throws at different speeds (Hirashima et al., 2007). As in the horizontal arm swing, however, elbow extension in overarm throws was found to be a major contributor to endpoint velocity at ball release. Although we found signs of small positive contributions to endpoint velocity from left elbow extension at estimated impact, only negative contributions from the corresponding right arm DOF were revealed. The orientation of the right elbow relative to clubhead path was changing throughout the movement and time series data show positive contributions from elbow extension in earlier stages of the downswing (Figure 5 & 6 in Study III). The negative contributions from elbow extension through impact could be a consequence of the asymmetry and mechanical coupling between the left and right arm, and potentially, contributions from elbow extension would differ if the golf swing was to be performed with the right arm only.

In contrast to single-limb movements where endpoint velocity contribution and regulation previously have been studied, length of the endpoint path (Fig. 2) and shoulder range of motion (Neal et al., 1990), increase substantially with endpoint velocity. This might explain observations that torso twist contribution for both groups began at approximately 15%, 25%, and 35% of the downswing at the slow, medium and fast test conditions, respectively (top row, Figure 5 & 6 in Study III). The progressively later onset of torso twist contribution presumably reflects a spatial similarity. A similar pattern of progressively later onset was observed for the 3 shoulder rotations in the left chain of the model (middle row, Figure 5 & 6 in Study III).

4.2.2 Endpoint mobility

Previous results suggest that knowledge about the effect of potential limb configurations on inertial behavior in reaching (Cos et al., 2013), is acquired performing everyday tasks with similar movement constraints. Specific training would be expected to be necessary to acquire the corresponding proficiency in a striking task involving an implement. However, present results revealed no significant difference in endpoint mobility between the intermediate and advanced skill level, suggesting that knowledge about inertial behavior is acquired at an earlier stage of development. Configurations associated with an increase in degree of alignment between the major axis and path, higher eccentricity, and/or higher mobility along path could also be in conflict with the specific task goal. Therefore, regulation of endpoint mobility with skill level cannot be excluded for other similar tasks.

Although mobility is a function solely of the configuration of the body and implement, and not of the velocities, maximizing endpoint velocity at estimated impact could put additional constraints on the movement (Putnam, 1993). Therefore, the possibility for prioritizing configurations that optimize mobility might be reduced compared to when aiming for a submaximal endpoint velocity. Nevertheless, results showed that the major axis was better aligned with movement direction in the fast compared to the slow shot condition. However, the difference in magnitude was small and shot condition had no effect on eccentricity.

Invariant endpoint mobility among different speeds is also indicated by the presented time series data. Time normalized graphs of endpoint mobility along and normal to path (Figure 10) are equally representative for slow, medium and fast shot conditions. This result is somewhat surprising considering that an increase in endpoint velocity is associated with an increase in path length (Figure 9), a behavior that could influence the sequence of arm and club configurations. Possibly, invariant endpoint mobility is advantageous from a control point of view. However, the present results do not rule out the possibility that invariant endpoint mobility was an indirect effect of the CNS controlling some other factor influencing arm-club configuration.

.

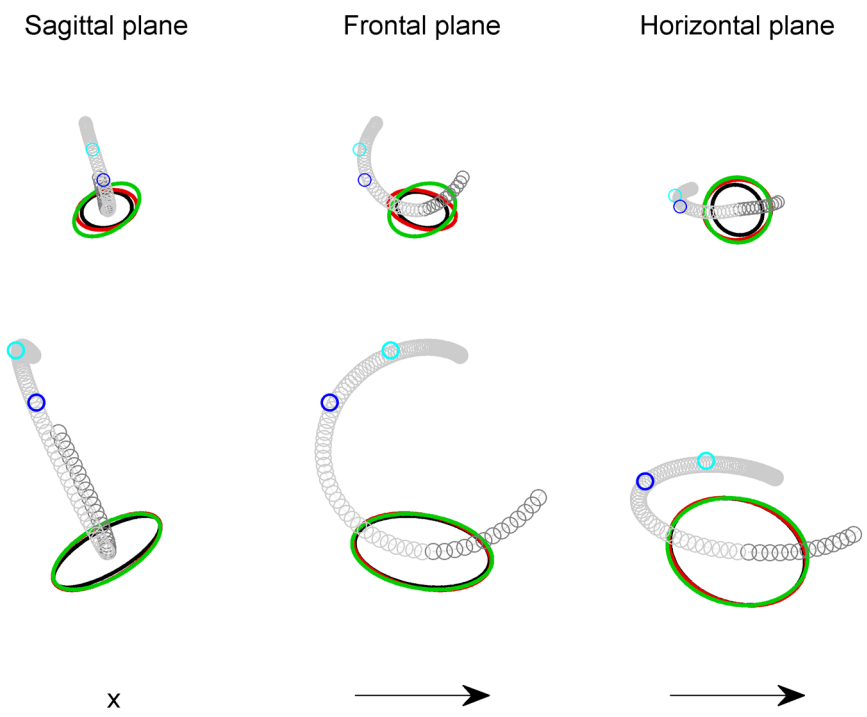

Figure 9 Mean endpoint mobility ellipses and mean endpoint movement paths for the fast test condition. Values for both groups are combined (n = 20). The upper row depicts ellipses and paths for the endpoint – grip center. The middle row depicts the corresponding variables for the endpoint – clubhead. Black ellipses are used for the model including both arms, red ellipses for the left arm model and green ellipses for the right arm model. Endpoint paths are grey before impact and dark grey after impact. Blue and magenta circles refer to top of backswing for slow and medium test conditions, respectively. The bottom row shows target direction.

In agreement with the leading joint hypothesis, the cost of active regulation of interaction torques (with muscle torque) has been found to have a strong effect on movement choice in arm movements (Dounskaia et al., 2011; Goble et al., 2007). Results in Study I showed a proximal-to-distal sequencing pattern in skilled golf swings to submaximal and maximal distances. This temporal relation accompanied with proximal-to-distal increments in segment angular speed indicated efficiently exploited interaction torques. If this would be the case, configurations that minimize both active regulation of interaction torques and inertial resistance parallel to endpoint path could exist in bimanual strikes with an implement. Such coexistence has neither been revealed in drawing nor reaching. Dounskaia et al. (2011) showed that directions of minimal active interference with interaction torque were perpendicular to directions of minimal inertial resistance in free-stroke drawing.

Perpendicular to directions of minimal active interference with interaction torque was also directions of maximal kinematic manipulability showing only a minor bias on movement choice (Dounskaia et al., 2011). Relatively large endpoint velocities suggest that kinematic manipulability might have a stronger influence on movement choice in bimanual striking.

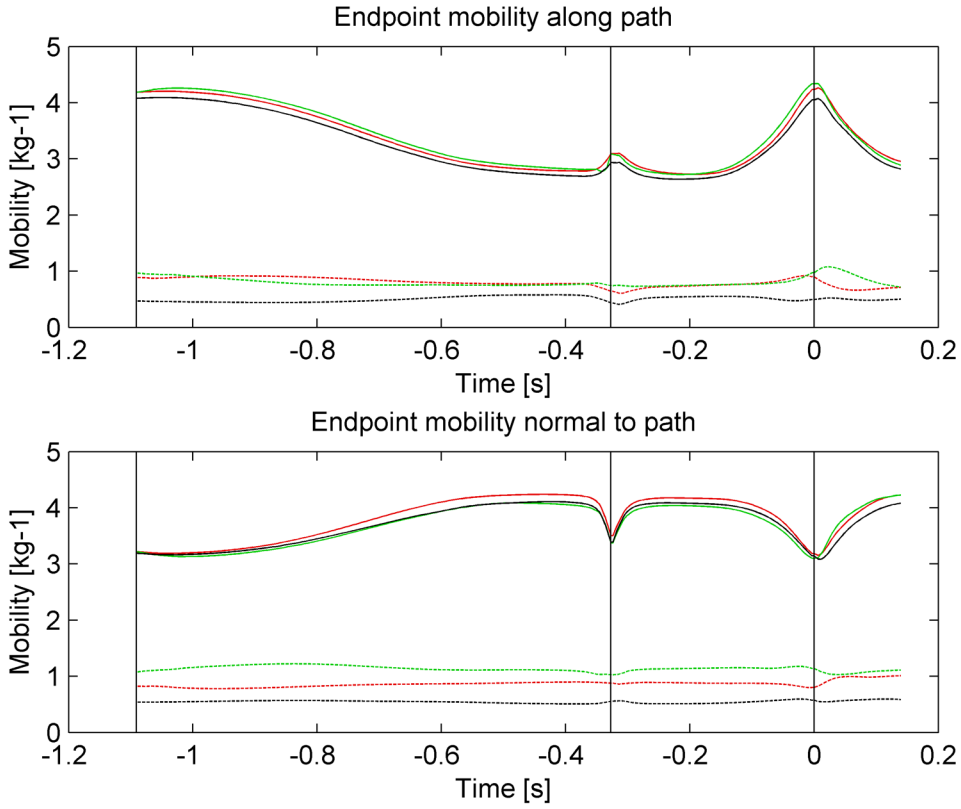

Figure 10 Mean mobility along and normal to path for endpoints grip center and clubhead. Black color represents the arm model including both arms. Red and green color represents the left and right arm models, respectively. Dashed lines represent time series data for the grip center and continuous lines represent the corresponding data for the clubhead. Vertical annotation lines are located at: movement onset; end of backswing; and at estimated impact (time = 0).

In summary, Study III adds support to the notion that intrinsic factors with anisotropy have strong influence on movement characteristics. The results suggest a deliberate strategy varying the length of endpoint path by changing the amount of rotation in proximally located joints, whilst keeping both arm-club configuration and inertial behavior of the endpoint approximately invariant among velocities at analogous endpoint positions and during the entire movement duration, respectively. This strategy was likely chosen to facilitate both endpoint velocity regulation (by the use of an invariant subset of joint rotations) as well as promoting spatial accuracy of the endpoint at ball impact.

5 FUTURE PERSPECTIVES

The LJH has been tested predominantly in reaching tasks with one arm, thus *leading* and *subordinate joints* have not been identified for manipulation tasks involving a closed chain of linked segments. Future research on golf ball striking may reveal whether the LJH can be expanded beyond the notion of a single joint as the leading component of limb motion. Typically, the *leading* and *subordinate* joints are separated by contrasting the contribution of torque generated by active MUS and passive INT to NET. In order to make the control of intersegmental dynamics in bimanual striking transparent, the possibility of using pressure mapping of the right hand together with inverse dynamics calculations for the golf club should be further explored. An alternative could be to compare joint acceleration and joint acceleration induced by interaction torques only. Such analysis could also be supplemented with data on muscle activation patterns.

This thesis shows how models including either one or two limbs compare, when studying endpoint control in skilled golf players that perform golf shots involving both arms. However, the study of skilled golf ball striking among one-armed golfers should provide further insight about unique adaptations to the control strategy that long-term training of either single-or double-handed manipulation might induce. Moreover, present results (Study III) suggest a deliberate strategy keeping endpoint mobility invariant among shot conditions. This could be further explored by manipulating the inertial parameters of the end-link.

6 ACKNOWLEDGEMENTS

First of all, my supervisors Toni Arndt, Maria Ekblom and Kjartan Halvorsen for providing invaluable support, knowledge and guidance. You allowed me to explore the areas I found most interesting.

A special acknowledgement to Alf Thorstensson for his encouragement and for giving me the opportunity to become part of the research group at The Laboratory of Biomechanics and Motor Control.

All colleagues in the BMC laboratory and in particular the contributions from Olga Tarassova and Johanna Rosén in Study IV are gratefully acknowledged.

John Hellström for introducing me to the game of golf many years ago. Your collaboration and friendship is appreciated.

Johnny Nilsson for getting me interested in research during my undergraduate studies.

Family and friends (I now actually may have time to meet some of you) for your encouragement and support.

Financial support by The Swedish School of Sport and Health Sciences, GIH, Stockholm, Sweden, and the Swedish National Centre for Research in Sports is acknowledged.

Movement recordings in study I and III were conducted in collaboration with The Swedish Golf Federation. The support is gratefully acknowledged.

Martin Petterson and Daniel Rosendahl for assisting in the recruitment of golf players.

Last but not least, all golf players participating in the studies of this thesis.

7 REFERENCES

Ambike, S., Schmiedeler, J.P., 2013. The leading joint hypothesis for spatial reaching arm motions. Exp Brain Res 224, 591-603.

Anderson, B.D.O., Moore, J.B., 1979. Optimal filtering. Prentice-Hall Englewood Cliffs, NJ.

Bland, J.M., Altman, D.G., 1986. Statistical methods for assessing agreement between two methods of clinical measurement. Lancet 1, 307-310.

Burden, A.M., Grimshaw, P.N., Wallace, E.S., 1998. Hip and shoulder rotations during the golf swing of sub-10 handicap players. J Sports Sci 16, 165-176.

Cheetham, P., Martin, P., Mottram, R., St Laurent, B., 2001. The Importance of Stretching the X-Factor in the Downswing of Golf, in: Thomas, P.R. (Ed.), Optimizing Performance in Golf. Australian Academic Press Pty. Ltd., Brisbane, pp. 192-199.

Coleman, S., Anderson, D., 2007. An examination of the planar nature of golf club motion in the swings of experienced players. J Sports Sci 25, 739-748.

Coleman, S.G., Rankin, A.J., 2005. A three-dimensional examination of the planar nature of the golf swing. J Sports Sci 23, 227-234.

Cos, I., Belanger, N., Cisek, P., 2011. The influence of predicted arm biomechanics on decision making. Journal of Neurophysiology 105, 3022-3033.

Cos, I., Khamassi, M., Girard, B., 2013. Modelling the learning of biomechanics and visual planning for decision-making of motor actions. Journal of physiology, Paris 107, 399-408.

Cos, I., Medleg, F., Cisek, P., 2012. The modulatory influence of end-point controllability on decisions between actions. J Neurophysiol 108, 1764-1780.

de Leva, P., 1996. Adjustments to Zatsiorsky-Seluyanov's segment inertia parameters. J Biomech 29, 1223-1230.

Dounskaia, N., 2005. The internal model and the leading joint hypothesis: implications for control of multi-joint movements. Exp Brain Res 166, 1-16.

Dounskaia, N., 2010. Control of human limb movements: the leading joint hypothesis and its practical applications. Exerc Sport Sci Rev 38, 201-208.

Dounskaia, N., Goble, J.A., Wang, W., 2011. The role of intrinsic factors in control of arm movement direction: implications from directional preferences. J Neurophysiol 105, 999-1010.

Franklin, D.W., Wolpert, D.M., 2011. Computational mechanisms of sensorimotor control. Neuron 72, 425-442.

Fujimoto-Kanatani, K., 1995. Determining the Essential Elements of Golf Swings Used by Elite Golfers [dissertation]. Corvallis (OR): Oregon State University.

Furuya, S., Kinoshita, H., 2007. Roles of proximal-to-distal sequential organization of the upper limb segments in striking the keys by expert pianists. Neurosci Lett 421, 264-269.

Galloway, J.C., Koshland, G.F., 2002. General coordination of shoulder, elbow and wrist dynamics during multijoint arm movements. Exp Brain Res 142, 163-180.

Goble, J.A., Zhang, Y., Shimansky, Y., Sharma, S., Dounskaia, N.V., 2007. Directional biases reveal utilization of arm's biomechanical properties for optimization of motor behavior. J Neurophysiol 98, 1240-1252.

Halvorsen, K., Johnston, C., Back, W., Stokes, V., Lanshammar, H., 2008. Tracking the motion of hidden segments using kinematic constraints and Kalman filtering. J Biomech Eng 130, 011012.

Hamilton, A.F., Jones, K.E., Wolpert, D.M., 2004. The scaling of motor noise with muscle strength and motor unit number in humans. Exp Brain Res 157, 417-430.

Harris, C.M., Wolpert, D.M., 1998. Signal-dependent noise determines motor planning. Nature 394, 780-784.

Hirashima, M., Kudo, K., Ohtsuki, T., 2003. Utilization and compensation of interaction torques during ball-throwing movements. J Neurophysiol 89, 1784-1796.

Hirashima, M., Kudo, K., Watarai, K., Ohtsuki, T., 2007. Control of 3D limb dynamics in unconstrained overarm throws of different speeds performed by skilled baseball players. J Neurophysiol 97, 680-691.

Hirashima, M., Yamane, K., Nakamura, Y., Ohtsuki, T., 2008. Kinetic chain of overarm throwing in terms of joint rotations revealed by induced acceleration analysis. J Biomech 41, 2874-2883.

Hogan, N., 1984. Adaptive control of mechanical impedance by coactivation of antagonist muscles. Automatic Control, IEEE Transactions on 29, 681-690.

Hogan, N., 1985. Impedance control: An approach to manipulation: Part II—Implementation. Journal of dynamic systems, measurement, and control 107, 8-16.

Jones, K.E., Hamilton, A.F., Wolpert, D.M., 2002. Sources of signal-dependent noise during isometric force production. J Neurophysiol 88, 1533-1544.

Kandel, E., 2013. Principles of Neural Science, Fifth Edition. McGraw-Hill Education.

Kim, Y.K., Hinrichs, R.N., Dounskaia, N., 2009. Multicomponent control strategy underlying production of maximal hand velocity during horizontal arm swing. J Neurophysiol 102, 2889-2899.

Kinzel, G.L., Hall, A.S., Jr., Hillberry, B.M., 1972. Measurement of the total motion between two body segments. I. Analytical development. J Biomech 5, 93-105.

Lemerle, P., Klinger, A., Cristalli, A., Geuder, M., 2008. Application of pressure mapping techniques to measure push and gripping forces with precision. Ergonomics 51, 168-191.

Milburn, P.D., 1982. Summation of segmental velocities in the golf swing. Med Sci Sports Exerc 14, 60-64.

Nafis, C., Jensen, V., Beauregard, L., Anderson, P., 2006. Method for estimating dynamic EM tracking accuracy of surgical navigation tools. SPIE Medical Imaging 2006 6141, 61410K-61416.

Neal, R., Abernethy, B., Moran, M., Parker, A., Year The influence of club length and shot distance on the temporal characteristics of the swings of expert and novice golfers. In Science and Golf: Proceedings of the First World Scientific Congress of Golf. St Andrews.

Putnam, C.A., 1993. Sequential motions of body segments in striking and throwing skills: descriptions and explanations. J Biomech 26 Suppl 1, 125-135.

Sabes, P.N., Jordan, M.I., 1997. Obstacle avoidance and a perturbation sensitivity model for motor planning. J Neurosci 17, 7119-7128.

Sabes, P.N., Jordan, M.I., Wolpert, D.M., 1998. The role of inertial sensitivity in motor planning. J Neurosci 18, 5948-5957.

van Beers, R.J., Haggard, P., Wolpert, D.M., 2004. The role of execution noise in movement variability. J Neurophysiol 91, 1050-1063.

Winter, D.A., 2005. Biomechanics and motor control of human movement, 3 ed. Wiley, Hoboken, N.J.

Woodworth, R.S., 1899. The accuracy of voluntary movement. Psychological Monographs 3, 1-114.

Yamasaki, H., Tagami, Y., Fujisawa, H., Hoshi, F., Nagasaki, H., 2008. Interaction torque contributes to planar reaching at slow speed. Biomed Eng Online 7, 27.

Zheng, N., Barrentine, S.W., Fleisig, G.S., Andrews, J.R., 2008. Swing kinematics for male and female pro golfers. Int J Sports Med 29, 965-970.